Applied Catalysis B: Environmental 89 (2009) 65–72

Contents lists available at ScienceDirect

Applied Catalysis B: Environmental

journal homepage: www.elsevier.com/locate/apcatb

Sintering and redispersion of platinum catalysts supported on tin oxide

Naoto Kamiuchi, Keiichi Taguchi, Toshiaki Matsui, Ryuji Kikuchi [1], Koichi Eguchi *

Department of Energy and Hydrocarbon Chemistry, Graduate School of Engineering, Kyoto University, Nishikyo-ku, Kyoto 615-8510, Japan

ARTICLE INFO

Article history:
Received 3 October 2008
Received in revised form 10 November 2008
Accepted 13 November 2008
Available online 27 November 2008

Keywords:
CO oxidation
Chemical interaction
Platinum
Tin oxide
Catalyst
Sintering
Dispersion
TEM

ABSTRACT

CO oxidation activities of platinum/tin oxide catalysts prepared by impregnation have been investigated in relation with their nano-structural changes in various reduction–oxidation treatments. Variously treated Pt/SnO_2 catalysts were characterized by XRD, XPS, and TEM. In 1 wt.% Pt/SnO_2 catalyst calcined at 400 °C, crystallized fine particles of Pt were highly dispersed on SnO_2 due to strong chemical interaction between two components. After the heat-treatment in a reducing atmosphere, the sintered Pt particles with grown size were frequently observed. Furthermore, unique texture of particles with core–shell structure was produced in the catalyst exposed in air after the reduction treatment at 400 °C. These large particles with the peculiar shape were re-dispersed by the reoxidation treatment at 400 °C to fine particle with similar size to the as-calcined catalysts. The reversibility of the microstructural changes between growth and redispersion of deposited particles was confirmed after the several reduction–oxidation cycles. It was revealed that the structural changes on the interface of Pt/SnO_2 catalysts were closely related to the catalytic activity for CO oxidation.

1. Introduction

Precious metal catalysts, such as platinum, palladium, ruthenium, and silver, have been applied for many chemical reactions so far because of their high catalytic activities. In some combinations of precious metals and support metal oxides, it is well-known that the drastic structural changes are induced by heat-treatment; i.e., one is well-known "sintering phenomenon" of metal particles. Sintering is accelerated at high temperatures, resulting in a deactivation of catalysts via reduction of active surface. The other phenomenon, "redispersion" of metal particles, opposes to the direction of minimization of surface energy. However, the redispersion has been reported in a few metal catalysts; e.g., Pt/Al_2O_3 [1–3], Rh/CeO_2 [4,5], $Re/\gamma\text{-}Al_2O_3$ [6–8], and Co/SiO_2 [9,10]. The proposed mechanisms for the redispersion differ from one catalyst to another, whereas this phenomenon is important for long catalyst life and reliability of the reactor. The mechanism of redispersion is often attributed to the difference in the chemical interaction between precious metal and support, depending on the combination of materials, the metal loading amount, the preparation method and so on.

Platinum/tin oxide, 1 wt.% Pt/SnO_2, catalysts exhibited higher catalytic activity for oxidation removal of Volatile Organic Compounds (VOCs) in spite of their smaller surface area (*ca.* 5 $m^2\,g^{-1}$) than conventional Pt/Al_2O_3 catalyst [11,12]. Another characteristic example for Pt/SnO_2 is its high activity for electrochemical oxidation of CO at a low oxidation potential. These favorable characteristics are expected to be originated from chemical interaction between platinum and tin oxide. The nano-structural change of 20 wt.% Pt/SnO_2 catalyst treated in various conditions was also investigated in order to elucidate the chemical interaction [13]. This heavily loaded catalyst allowed us to recognize the phase and morphological changes. However, it is of significant importance in relation to the actual catalytic reaction whether the practical loading catalyst such as 1 wt.% Pt/SnO_2 undergoes the microstructural changes with various thermal treatments in controlled atmosphere. In this paper, then, the nano-structure of 1 wt.% Pt/SnO_2 catalysts treated in several conditions was carefully studied. Especially, the sintering and redispersion process of Pt deposits, which was clearly observed for the low loading sample, was analyzed in relation to reduction–oxidation treatments.

2. Experimental

2.1. Catalyst preparation

The platinum catalysts supported on tin oxide powder with 1 wt.% and 20 wt.% platinum loading were prepared by the

* Corresponding author. Tel.: +81 75 383 2519; fax: +81 75 383 2520.
E-mail address: eguchi@scl.kyoto-u.ac.jp (K. Eguchi).
[1] Present address: Department of Chemical System Engineering, The University of Tokyo, 7-3-1 Hongo, Bunkyo-ku, Tokyo 113-8656, Japan.

0926-3373/$ – see front matter © 2008 Elsevier B.V. All rights reserved.
doi:10.1016/j.apcatb.2008.11.026

Table 1
Heat-treatment of Pt/SnO_2.

Sample name	Heat-treatment
S-1	As-calcined
S-2	Reduction[a] at 90 °C for 2 h
S-3	Reduction at 200 °C for 1 h
S-4	Reduction at 400 °C for 0.5 h
S-5	Reduction at 400 °C for 0.5 h, followed by oxidation[b]
S-4 II	Reduction at 400 °C for 0.5 h after the heat-treatment of S-5
S-5 II	Reoxidation[b] after the heat-treatment of S-4 II
S-4 V	Reduction at 400 °C for 0.5 h after the fourth consecutive reduction–reoxidation treatments
S-5 V	Reoxidation[b] after the heat-treatment of S-4 V

[a] Reduction atmosphere: 10% H_2/N_2.
[b] Oxidation was conducted in air at 400 °C for 0.5 h.

impregnation method. An aqueous solution of $Pt(NO_2)_2(NH_3)_2$ (Tanaka Kikinzoku Kogyo) and SnO_2 powder (Wako Pure Chemical Industries Ltd.) calcined at 800 °C for 5 h were used for Pt source and support, respectively. After immersing the SnO_2 powder to the solution, the mixture was kept on a steam bath at 80 °C until the solution was evaporated to dryness. The resulting powder was then heat-treated under various conditions (Table 1). In some cases, the reduction or reoxidation treatments were conducted repeatedly (2–5 times). The reduction and oxidation were carried out in 10% H_2/N_2 and in air, respectively.

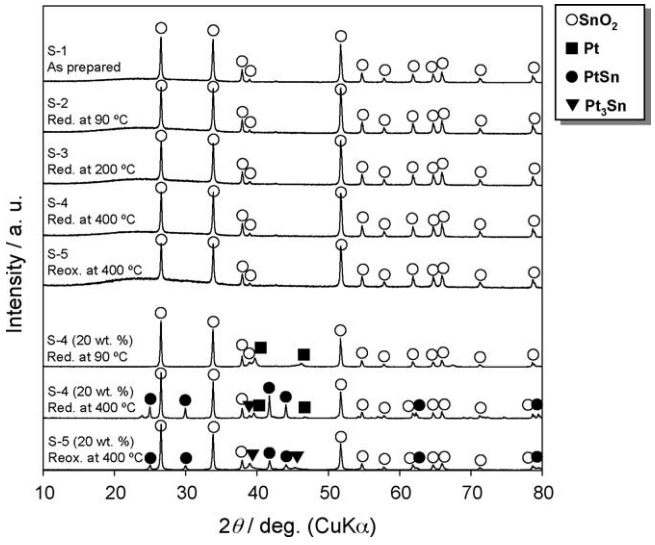

Fig. 1. XRD patterns of 1 wt.% Pt/SnO_2 (S-1–S-5) and 20 wt.% Pt/SnO_2 (S-2, S-4, and S-5): (○) SnO_2, (■) Pt, (●) PtSn, (▼) Pt_3Sn.

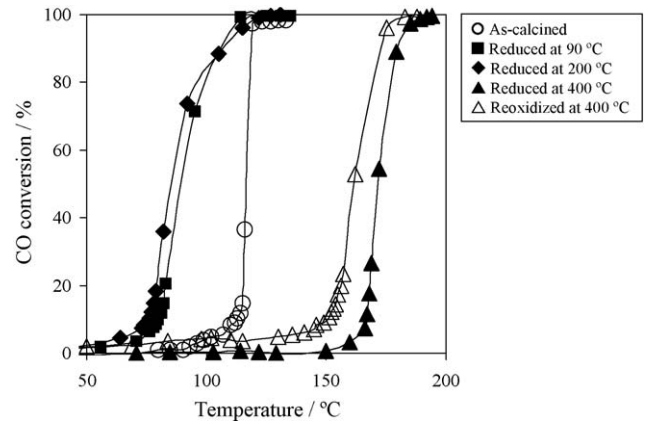

Fig. 2. Carbon monoxide conversion over 1 wt.% Pt/SnO_2. Reaction conditions: CO, 5.0%; O_2, 15.0%; N_2, balance; total flow rate = 80 ml/min; S.V. = 48,000 l kg^{-1} h^{-1}.

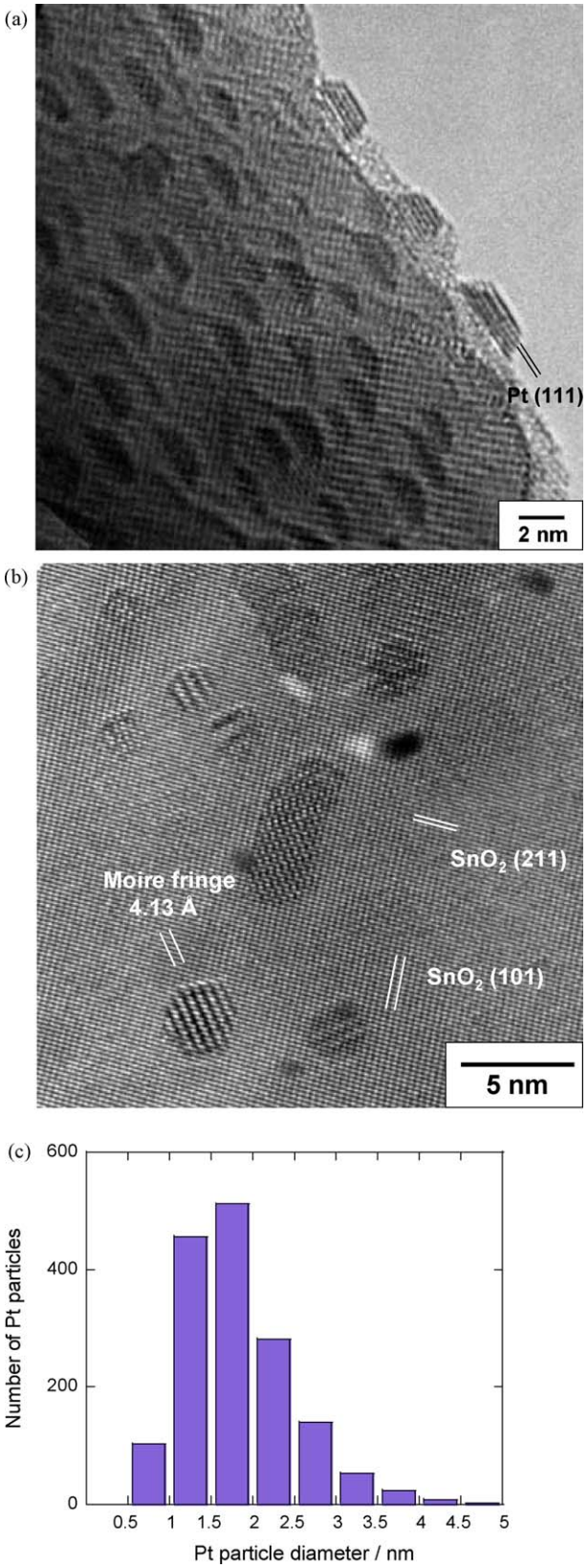

Fig. 3. TEM images and platinum particle size distribution of as-calcined 1 wt.% Pt/SnO_2 (S-1).

2.2. Catalytic oxidation of CO

A fixed-bed flow reactor made of quartz tubing of 8 mm inner diameter was used, and the prepared catalyst (100 mg) was set in the reactor. Each catalyst was tabletted and pulverized into 0.85–1.7 mm before catalytic reaction tests. A gaseous mixture composed of 5.0% CO, 15% O_2, and 80% N_2 was fed at a flow rate of 80 ml min^{-1} (space velocity: 48,000 l kg^{-1} h^{-1}). The outlet gas compositions were analyzed by an on-line non-dispersive infrared detector (NDIR, CGT-7000).

2.3. Catalyst characterization

The phases in resulting powders were characterized by X-ray diffraction (Rigaku Rint 1400 X-ray diffractometer with Cu Kα radiation). X-ray photoelectron spectroscopy (Shimadzu ESCA-850 with Mg Kα radiation) was carried out for the evaluation of the surface electronic state. To compensate sample charging, all spectra were measured with reference to the binding energy of C 1s core level line (285.0 eV). The high Pt loading catalysts of 20 wt.% Pt/SnO_2 were mainly used for the analysis of XPS to obtain sharp spectra, since the platinum loading of 1 wt.% was too small to observe well-resolved signals. The BET surface area of as-calcined catalyst was determined by N_2 adsorption at the liquid nitrogen temperature using a Shimadzu Gemini 2375 analyzer. The morphology and lattice images were observed by transmission electron microscopy using Hitachi H-9000 with LaB_6 electron source and Philips CM200 FEG equipped with a field emission electron gun.

3. Results and discussion

3.1. Characterization by XRD

The 1 wt.% Pt/SnO_2 sample (S-1) was reduced at three different temperatures (S-2, S-3, S-4), and subsequently reoxidized (S-5). The results of the X-ray diffraction for the catalysts (S-1–S-5) are shown in Fig. 1. Regardless of heat-treatment conditions, the diffraction pattern was identical to that of SnO_2 and the phases ascribable to the platinum-containing compounds were not detected in the course of reduction and oxidation treatments. The absence of metallic Pt line and unchanged XRD patterns should be due to the small loading amount. As will be suggested in the latter section, small size with thin stacking of atomic layers for the fine Pt deposits on the SnO_2 support is another reason for the unobservable Pt lines.

The phase appeared upon reduction treatment was unclear from the XRD pattern after the pretreatment because of the extremely weak diffraction from Pt species. Thus, the phase transformation was investigated by using 20 wt.% Pt/SnO_2 catalyst.

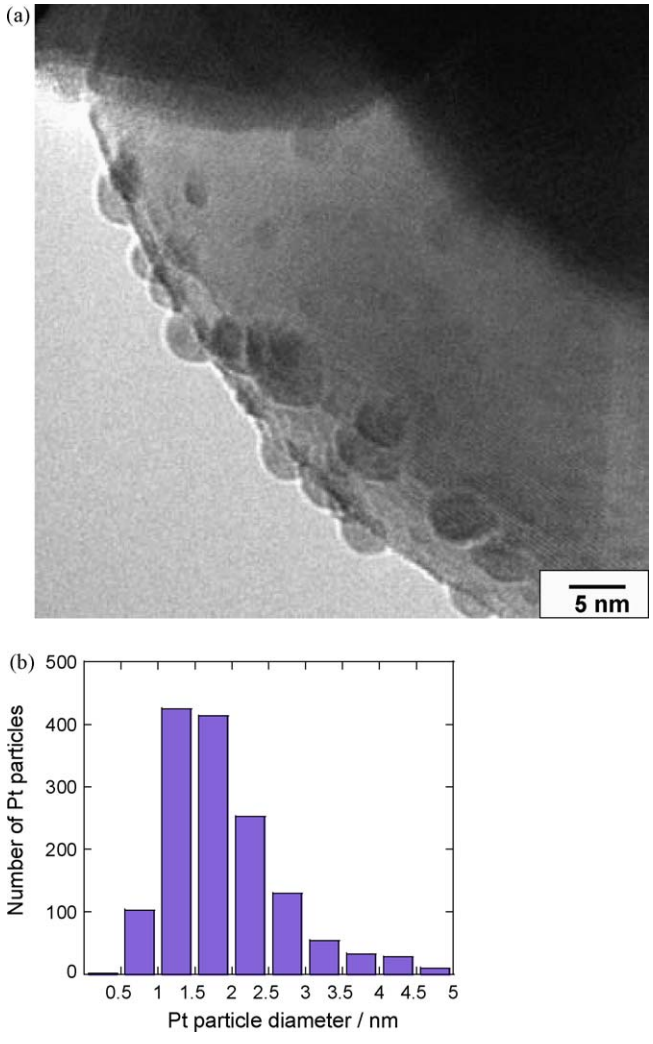

Fig. 4. TEM image and platinum particle size distribution of 1 wt.% Pt/SnO_2 reduced at 90 °C for 2 h in 10% H_2/N_2 (S-2).

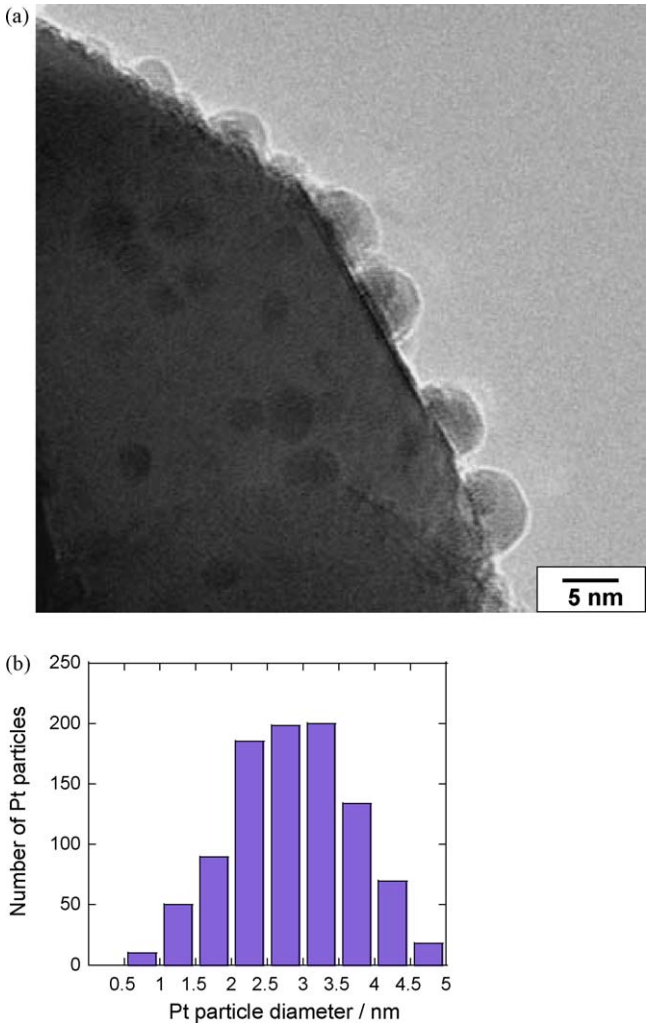

Fig. 5. TEM image and platinum particle size distribution of 1 wt.% Pt/SnO_2 reduced at 200 °C for 1 h in 10% H_2/N_2 (S-3).

The sample after reduction at 90 °C consisted of the lines from SnO_2 and metallic Pt phases. The reduced sample at 400 °C on the other hand, was attributed the mixture of SnO_2 and intermetallic compounds of PtSn and Pt_3Sn. These phases were formed upon reduction of tin oxide and solid state alloying. As seen in Fig. 1, the reoxidation of the reduced catalyst weakened the diffraction from the intermetallic compounds and tended to restore the metallic Pt lines. The direction of the solid state reactions have been clarified from the XRD of the heavy loaded Pt/SnO_2 sample, whereas the solid state reaction and phase separation should be very slow and incomplete due to large mass of metal deposits [13]. Therefore, the detailed microstructure and phase changes were analyzed by the TEM observation.

3.2. Catalytic activity of Pt/SnO_2 catalyst for CO oxidation

Catalytic activities of the 1 wt.% Pt/SnO_2 catalyst for CO oxidation were investigated after various reduction or oxidation treatments as shown in Fig. 2. Oxidation of CO started from *ca.* 90 °C for the as-calcined catalyst followed by a sharp rise in conversion up to 120 °C of complete oxidation. The oxidation temperature strongly depended on the pretreatment condition. The oxidation activity was enhanced after reduction pretreatment in H_2 at 90 °C or 200 °C. The light-off temperature was significantly reduced to 70 °C by these reduction treatments. The light-off temperature was low in spite of low overall surface area of the catalyst (*ca.* 5.4 $m^2\,g^{-1}$). On the other hand, the activity was suppressed with the reduction pretreatment at 400 °C. The reduced catalyst after heating in H_2 at 400 °C was further treated in oxygen at 400 °C. The reoxidation pretreatment recovered the activity to some extent. Thus the CO oxidation activity was very sensitive to the reduction and oxidation pretreatments.

As shown in Fig. 2 the high activity of Pt/SnO_2 for CO oxidation is quite attractive. It is generally known for other supported precious metal catalysts that the reduction treatment gives rise to enhancement of catalytic activity for CO oxidation. The improvement is ascribed to exposure of clean metallic surface which is active of CO adsorption and dissociation. The improvement of the activity after reduction pretreatment of Pt/SnO_2 at 90 °C and 200 °C is attributed to this effect. The deterioration of the activity with reduction at 400 °C is expected to the formation of the intermetallic compounds and aggregation of metal grains on the tin oxide surface. It indicates that the bare surface of Pt metal is more active than the oxidized Pt or intermetallic compound surfaces. The reoxidation treatment of reduced Pt restored the CO oxidation activity to some extent. The improvement of the CO oxidation activity by the reoxidation treatment is small in extent. This is because the reoxidation treatment is not enough. If the catalyst reduced at 400 °C is reoxidized at 400 °C for longer time,

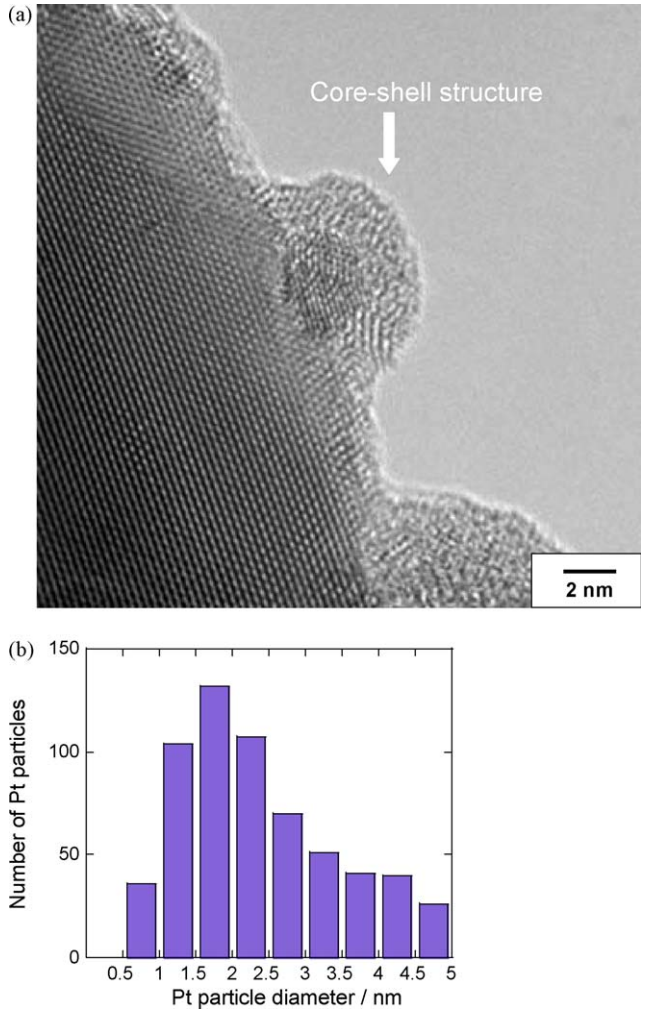

Fig. 6. TEM image and platinum particle size distribution of 1 wt.% Pt/SnO_2 reduced at 400 °C for 0.5 h in 10% H_2/N_2 (S-4).

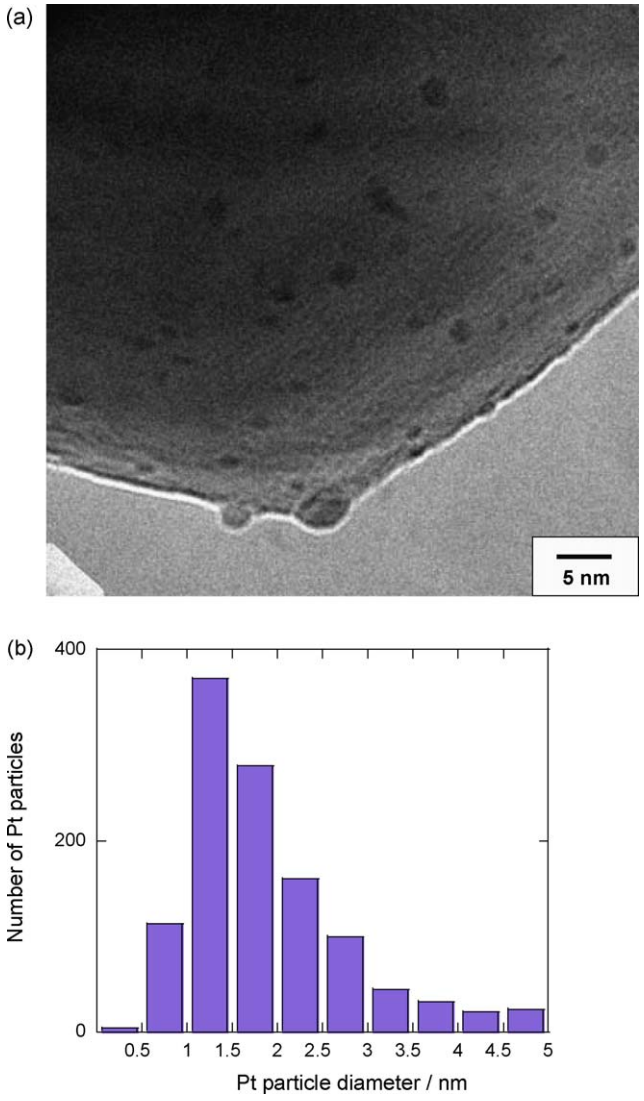

Fig. 7. TEM image and platinum particle size distribution of 1 wt.% Pt/SnO_2 reoxidized at 400 °C for 0.5 h (S-5) after the reduction treatment at 400 °C.

Table 2
Binding energy of Pt 4f and Sn 3d photoelectron spectra of 20 wt.% Pt/SnO_2.

Sample name	Binding energy (eV)	
	Pt $4f_{7/2}$	Sn $3d_{5/2}$
S-1	74.3	486.6
S-2	71.3	487.1
S-3	71.1	487.1
S-4	71.1	487.1
S-5	74.3	486.9

Table 3
Number average particle diameters of all Pt/SnO_2 catalyst.

Sample name	Average particle diameter (nm)
S-1	1.9
S-2	2.0
S-3	3.1
S-4	3.7
S-5	2.0
S-4 II	4.6
S-5 II	1.8
S-4 V	4.8
S-5 V	2.3

the catalytic activity will be comparable to that of the as-calcined one. This activity recovery is expected to the morphological change and exposure of metallic Pt fine particles as will be discussed from the TEM observations of Pt/SnO_2 after reduction and oxidation treatments.

3.3. Surface analysis by XPS

The binding energies of Pt 4f and Sn 3d in 20 wt.% Pt/SnO_2 (S-1–S-5) were measured by X-ray photoelectron spectroscopy (Table 2). The Pt signals for 1 wt.% Pt/SnO_2 sample was too weak to evaluate the oxidation state. In the case of as-calcined catalyst (S-1), the binding energy of Pt $4f_{7/2}$ and Sn $3d_{5/2}$ were 74.3 eV and 486.6 eV, respectively. Thus the both Pt and Sn elements are oxidized in the initial state. In contrast, the reduced Pt/SnO_2 catalysts at 90 °C (S-2) exhibited the binding energies of metallic platinum, whereas the oxidized state of tin was unchanged. The metallic Pt and Sn oxide states are stable up to the reduction at 400 °C from XPS (S-3 and S-4). The surface of SnO_2 particles will be reduced to metallic Sn or SnO_x after the reduction treatments at high temperature such as 200 °C and 400 °C. However, only SnO_2 was confirmed in the reduced sample. This is because the metallic Sn or SnO_x was oxidized to SnO_2 soon after the reduced sample was exposed to air. In Pt/SnO_2 catalyst re-oxidized at 400 °C (S-5), the oxidation state of platinum and tin oxide was restored being judged from the binding energies of Pt $4f_{7/2}$ and Sn $3d_{5/2}$ comparable to these of S-1.

3.4. Microscopic observation of 1 wt.% Pt/SnO_2 catalyst calcined

TEM images and the platinum particle size distribution estimated from the images of S-1 are shown in Fig. 3. The number average particle diameters are summarized in Table 3. Platinum particles were highly dispersed on the surface of SnO_2 support (Fig. 3(a)), and the average particle size was evaluated to be *ca.* 1.9 nm. Although a number of fine islands of Pt were observed, the boundaries between Pt deposits and tin oxide surface were poorly defined from the contrast and the continuous lattice array. This image suggests the intimate interaction between platinum and SnO_2. The lattice arrays of Pt in fine deposits were well-fitted to

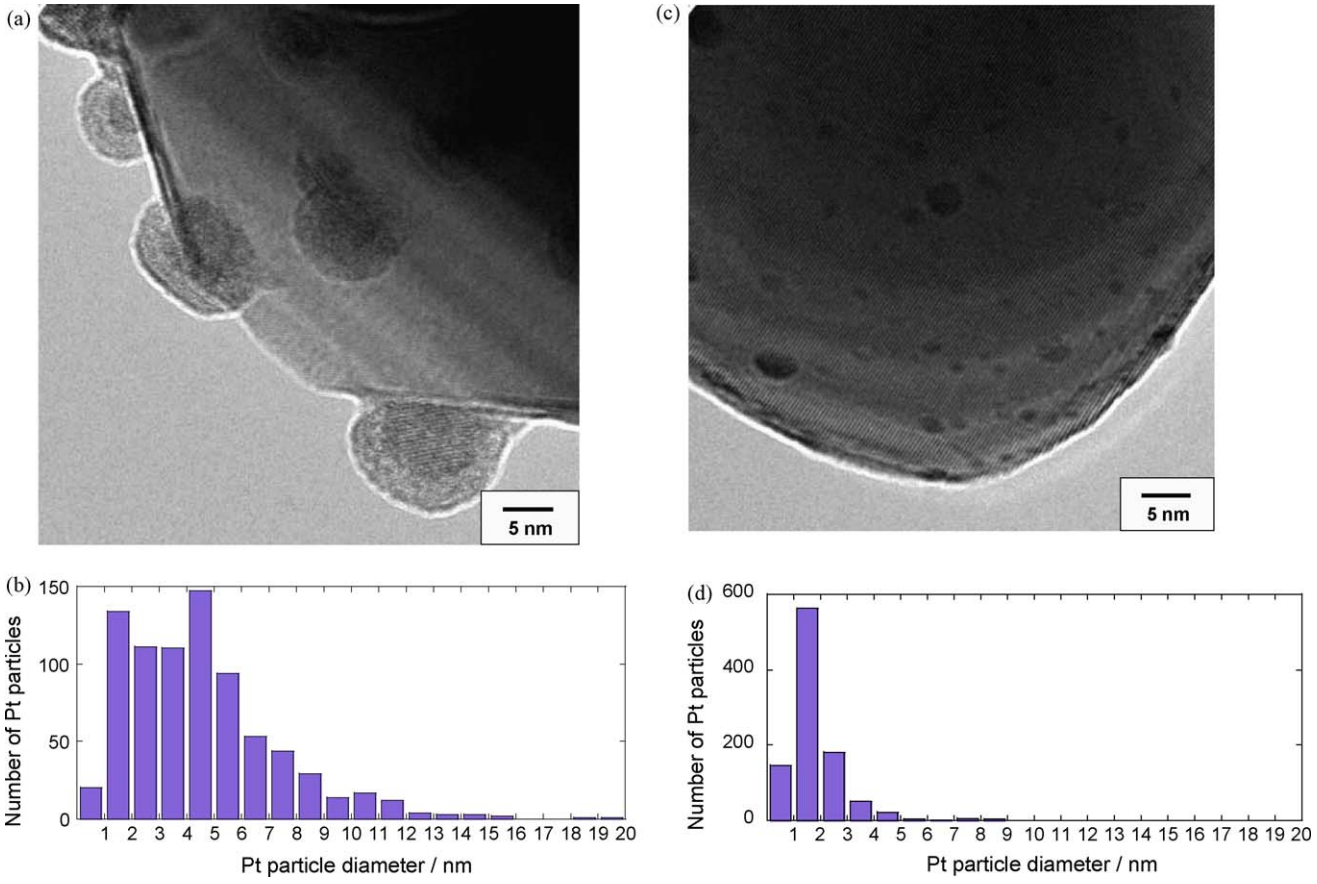

Fig. 8. TEM images and particle size distributions of 1 wt.% Pt/SnO_2 after twice consecutive reduction–reoxidation heat-treatments ((a), (b): S-4 II, (c), (d): S-5 II).

those of tin oxide. The morphology of the platinum was platelet deposits on the tin oxide surface with a few atomic layers stacking. The fine crystallite size and in sufficient layer stacking appear to be the reason for unobservable X-ray lines of Pt. It was also revealed that platinum particles with hexagonal shape were deposited on SnO_2 as can be seen in the surface view image of Fig. 3(b). This hexagonal profile of deposits indicates that the platinum particles are exposing their surface with low index planes as reported in the other catalysts such as Au/TiO_2 [14]. In addition, the Moiré fringes attributed to overlapping platinum and SnO_2 lattice images with pattern spacing of *ca.* 4.1 Å were observed. The direction of the Moiré fringes for different platinum particles on the SnO_2 particle agreed with each other. Therefore, platinum particles will glow in the particular orientation with the strong interaction on the topmost surface of the SnO_2 support. It was mentioned in the previous section, the platinum species in S-1 were in the oxidation state. The lattice fringe of fine particles in Fig. 3(a), however, was attributed to Pt(1 1 1), suggesting that the particles were in the metallic state. This discrepancy between XPS data and TEM images can be explained by as follows. One reason is the difference in the platinum loading amount. In the case of the 20 wt.% Pt/SnO_2 catalyst used for XPS analysis, the platinum particles were larger than those in the 1 wt.% Pt/SnO_2 catalyst. Thus, the interaction between platinum and SnO_2 in the 20 wt.% Pt/SnO_2 catalyst was weak for the Pt atoms located away from the interface. Thus, oxidation of top surface of platinum was facilitated. The second possible reason is that the electronic state of platinum particles with the size of *ca.* 3 nm may be influenced by quantum size effect (QSE). The last reason may be the extra-atomic relaxation [15,16]. The electrons belonging to the neighboring atoms to the central cation occupy the core hole on relaxation which is created in ejecting the photoelectron for XPS analysis. When this relaxation proceeds, however, the extra-atomic relaxation cannot explain why the chemical sift occurs only in the calcined catalyst (S-1). Therefore, the oxidation of top surface of Pt particles and QSE are more plausible reasons.

3.5. The effect of reduction

The TEM images and the platinum particle size distributions of S-2 and S-3, treated in a hydrogen atmosphere at 90 °C and 200 °C, are shown in Figs. 4 and 5, respectively. For the sample of S-2 reduced at 90 °C in 10% H_2/N_2, the size of platinum particle was *ca.* 2.0 nm, which was comparable to that of S-1 (Fig. 4(b)). However, most of platinum particles were in hemispherical shape, which was obviously different from the shape of Pt in S-1 (Fig. 4(a)). Thus, the heat-treatment in hydrogen induced the drastic change in the interfacial interaction between platinum and tin oxide. After reduction at 200 °C, platinum particles in the sample of S-3 were grown to the size of *ca.* 3.1 nm (Fig. 5(b)). The pretreatment in a reducing atmosphere at higher temperature accelerated the aggregation of platinum particles. Two mechanisms for the catalyst sintering have been proposed so far; i.e., one is "Ostwald ripening (OR)", and the other is "particle migration and coalescence (PMC)" [17–19]. In the OR mechanism, the growth of metal particles on the support proceeds by the migration of metal atoms or clusters through the gas phase or the surface of the support. On the other hand, for the platinum particles on reduced tin oxide surface at elevated temperatures modified PMC mechanism appears to be operative; i.e., the particle growth proceeds by the surface diffusion and collision of the metal particles. The particles should be grown in the form of the intermetallic compounds. The vaporization of Pt species was expected to be suppressed in the binary metal.

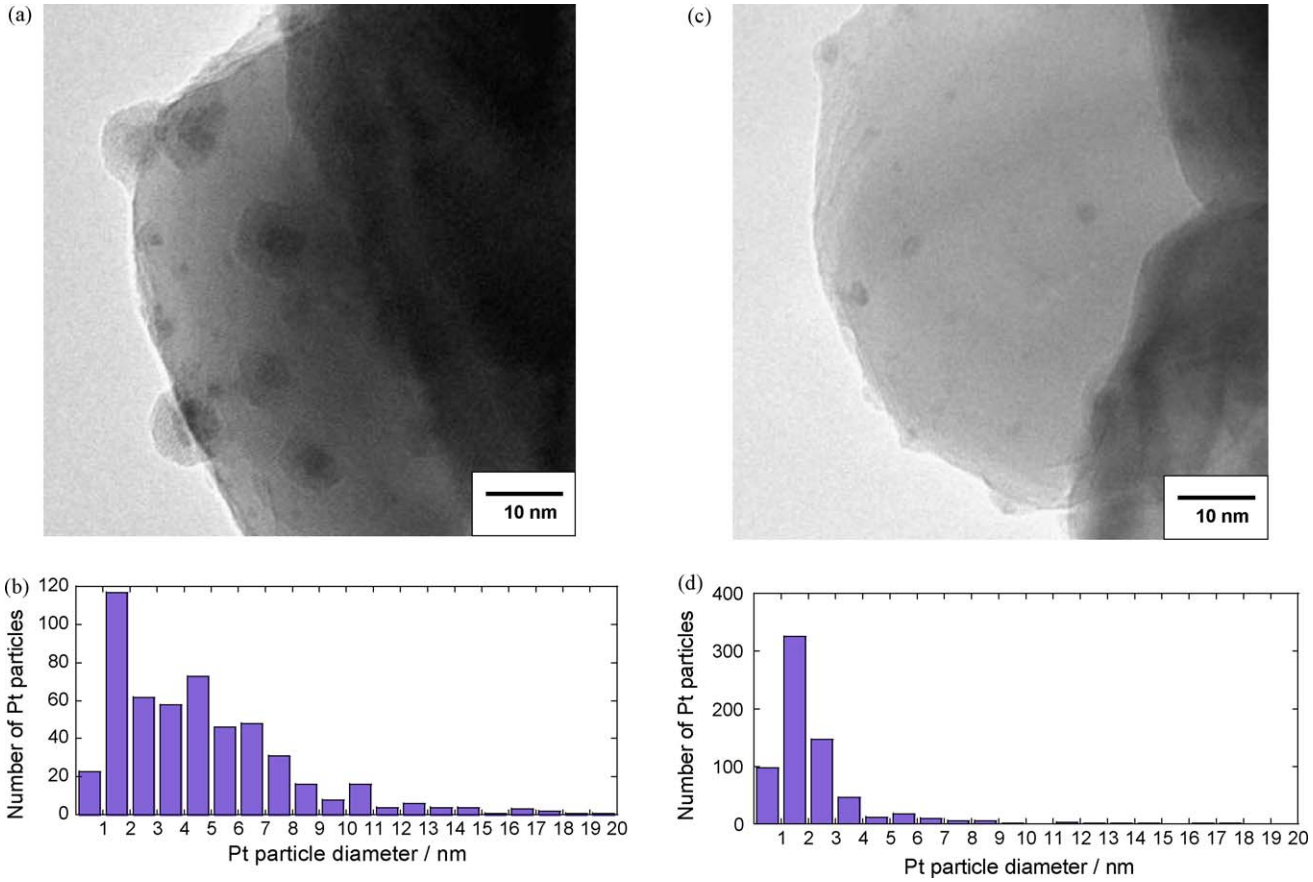

Fig. 9. TEM images and particle size distributions of 1 wt.% Pt/SnO_2 after fifth consecutive reduction–reoxidation heat-treatments ((a), (b): S-4 V, (c), (d): S-5 V).

Fig. 6(a) illustrates TEM photograph of the S-4 sample reduced at 400 °C in a hydrogen atmosphere, and Fig. 6(b) shows the distribution of the particle size on SnO_2 support in the S-4 sample. The average size of particles was *ca.* 3.7 nm. The particle growth has been accelerated by the reduction at elevated temperatures of 400 °C. It is noted that the platinum deposits possessed the core–shell structure (Fig. 6(a)). The core part was well-crystallized, whereas the shell part was in an amorphous state. The most stable species for the Pt–Sn system are intermetallic compounds of PtSn and Pt_3Sn in reducing atmosphere. The same reaction should proceed for the fine Pt deposits on 1 wt.% Pt, though XRD is not sensitive enough to evidence the formation of the fine binary metal. The core–shell structure was formed by the phase separation of oxidized Sn species from the particles of the intermetallic compounds such as PtSn or Pt_3Sn in mild oxidizing atmosphere on exposure to air. In our recent experiments, the adsorption of CO was too small to be observed up to 20 wt.% Pt loading in the Pt/SnO_2 catalysts reduced at 400 °C [20]. It is expected that the shell part, such as the layer of tin oxide, inhibits the CO adsorption on the top surface of the platinum based particles. It has been also reported that the Pt/SnO_2 catalysts reduced at 200 °C were active for elctrocatalytic oxidation of CO with lower onset potential than that of Pt/C [21,22].

3.6. The effect of reoxidation

The structural change induced by the reoxidation treatment at 400 °C for the 1 wt.% Pt/SnO_2 catalyst was investigated. The S-4 sample was reoxidized at 400 °C in air, and the resulting powder was indexed as S-5. TEM photograph and the particle size distribution of S-5 are shown in Fig. 7. From these results, it was revealed that fine particles with the average size of *ca.* 2.0 nm were restored. This microstructural change suggests redispersion of metallic Pt particles. The mean size of particles was smaller than that of S-4 and comparable to that of S-1. It has been previously reported for 1 wt.% Pt/SnO_2 catalyst that the catalytic oxidation activity was enhanced with oxidation pretreatment. Thus, the S-5 sample with fine Pt deposits exhibited higher catalytic activity for the catalytic oxidation of VOCs than the reduced samples [11]. The promotion by reoxidation treatment was also observed for CO oxidation in Fig. 2. In the case of 20 wt.% Pt/SnO_2, the complete recovery of metallic platinum particles from the intermetallic phase was observed only after the reoxidation at 800 °C [13]. Although such elevated temperatures are required for complete reduction on large grains, sintering of metallic Pt concurrently proceeded. On the other hand, the clear evidence of redispersion in 1 wt.% Pt/SnO_2 catalyst was observed even at 400 °C, since the particles in 1 wt.% Pt/SnO_2 were small enough to facilitate the rapid textural changes with the reduction–oxidation treatments.

3.7. Reproducibility of the effects caused by reduction–oxidation treatment

As mentioned above, the sintering and redispersion behavior of platinum particles was verified by the repeated cycles of reduction–reoxidation treatments. Then, the reproducibility of structural change was examined for the S-5 sample. The "S-4 II" catalyst was defined as the catalyst reduced at 400 °C after the first reduction–oxidation treatment at 400 °C. Then, S-4 II was subsequently reoxidized at 400 °C, and the resultant sample was denoted as "S-5 II". In the same way, "S-4 V" and "S-5 V" samples corresponds to the samples subjected to the fifth consecutive reduction and oxidation treatments, respectively. TEM images and particle size distributions of S-4 II and S-5 II are shown in Fig. 8, and those of S-4 V and S-5 V are summarized in Fig. 9. In S-4 II and S-4 V, many particles with the core–shell structure are observed like in S-4 (Figs. 8(a) and 9(a)). These particles have been grown during heating at high temperatures. The core–shell structure resulted from oxidation of the particles and subsequent phase separation as in sample S-4 after single reduction treatment. The average sizes of those particles were 4.6 nm and 4.8 nm in S-4 II and S-4 V, respectively, as shown in Figs. 8(b) and 9(b). These values were a little larger than that of S-4 (3.7 nm). The mean particle diameters of S-5 II and S-5 V were 1.8 nm and 2.3 nm, respectively (Figs. 8(d) and 9(d)), which were comparable to those of S-1 and S-5. These results indicated that the sintered platinum particles were reversibly dispersed by the oxidation treatment at 400 °C. Thus, this reoxidation treatment is suggested to be the effective method to regenerate Pt/SnO_2 catalyst degraded by the particle growth.

In 20 wt.% Pt/SnO_2 reoxidized at 400 °C in air for five times (S-5 V), the amorphous particles with characteristic morphology were observed as shown in Fig. 10. The large tin oxide particles include some embedded Pt crystallites with the size of 1–2 nm, as

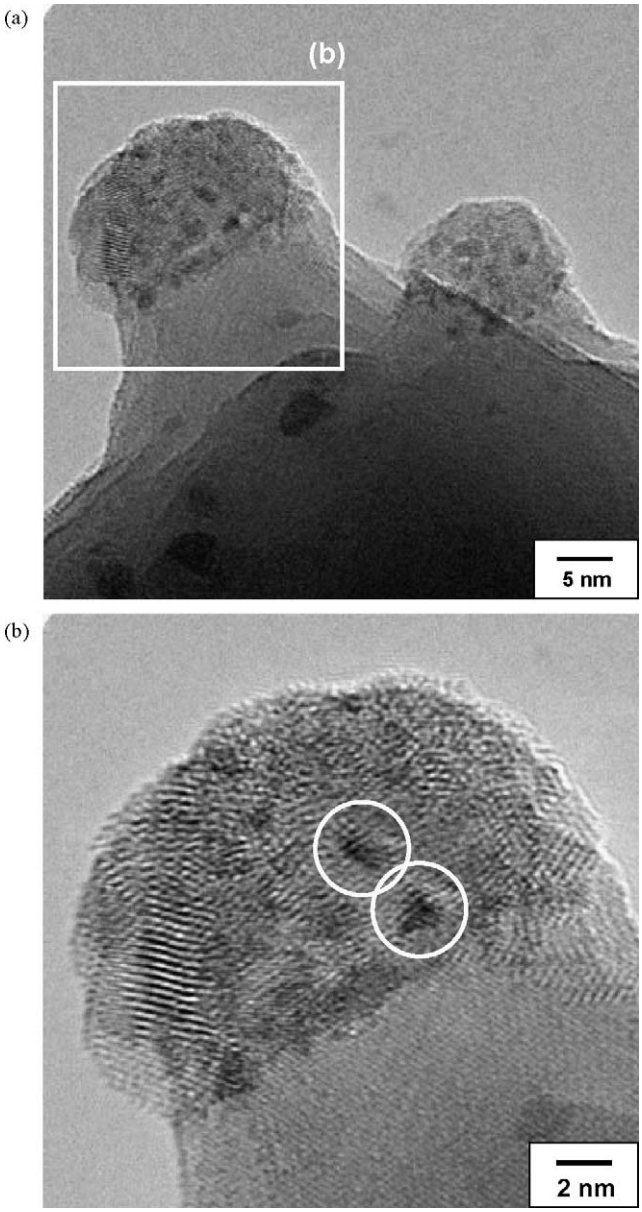

Fig. 10. TEM images of 20 wt.% Pt/SnO_2 catalyst after fifth consecutive reduction–reoxidation heat-treatments (S-5 V).

indicated by circles. Since these crystallites were formed by reoxidation at 400 °C, they appear to be in the intermediate state for the redispersion of metallic Pt crystallites. Then, the redispersion mechanism of platinum particles is proposed as follows; the intermetallic compound particles such as PtSn and Pt_3Sn are decomposed to nanosized platinum crystallites by the reoxidation treatment at 400 °C. The amorphous tin oxide surrounding the platinum crystallites diffuses to grow on the support particles, and the platinum crystallites emerge to the surface. The deposition of fine Pt crystals by the phase separation should be the reason for the redispersion and restored catalytic activity.

4. Conclusions

The structural changes in 1 wt.% Pt/SnO_2 catalysts treated under several conditions were investigated by TEM observation, and the results were compared with the catalytic activity for CO oxidation. The aggregation of platinum particles was induced by the reduction treatment. The particles with the peculiar "core–shell structure" were observed in the catalysts exposed in air after the reduction treatment at 400 °C. The formation of this structure was clearly explained by the phase separation of tin oxide or sub-oxide phase from the intermetallic compound particles under a mild oxidation atmosphere. Moreover, it was suggested that the redispersion of platinum particles will be initiated by the decomposition of the particles with core–shell structure after the reoxidation treatment at 400 °C. The reproducibility of these structural changes between growth and redispersion of deposited particles was verified by TEM observation for the catalysts heat-treated repeatedly in reducing and oxidizing atmospheres. This unusual nature derived from the strong chemical interaction may be operative for some combination of precious metals and reducible oxides. Especially, modification of catalytic activity and redispersion with reduction or oxidation treatment should be important for the regeneration of the deactivated catalysts, as seen in the results of CO oxidation.

Acknowledgment

This work was supported by Core Research for Evolutional Science and Technology (CREST) of Japan Science and Technology Agency (JST).

References

[1] T.J. Lee, Y.G. Kim, J. Catal. 90 (1984) 279.
[2] F.L. Normand, J. Phys. Chem. 100 (1996) 9068.
[3] A. Monzon, T.F. Garetto, A. Borgna, Appl. Catal. A: Gen. 248 (2003) 279.
[4] S. Bernal, F.J. Botana, J.J. Calvino, G.A. Cifredo, J.A. Pérez-Omil, J.M. Pintado, Catal. Today 23 (1995) 219.
[5] S. Bernal, J.J. Calvino, M.A. Cauqui, J.A. Pérez-Omil, J.M. Pintado, J.M. Rodríguez-Izquierdo, Appl. Catal. B: Environ. 16 (1998) 127.
[6] J. Okal, H. Kubicka, L. Kepinski, L. Krajczyk, Appl. Catal. A: Gen. 162 (1997) 161.
[7] J. Okal, L. Kepinski, L. Krajczyk, M. Drozd, J. Catal. 188 (1999) 140.
[8] J. Okal, L. Kepinski, L. Krajczyk, W. Tylus, J. Catal. 219 (2003) 362.
[9] D. Potoczna-Petru, J.M. Jablonski, J. Okal, L. Krajczyk, Appl. Catal. A: Gen. 175 (1998) 113.
[10] D. Potoczna-Petru, L. Kepinski, Catal. Lett. 9 (1991) 355.
[11] T. Mitsui, K. Tsutsui, T. Matsui, R. Kikuchi, K. Eguchi, Appl. Catal. B: Environ. 78 (2008) 158.
[12] T. Mitsui, K. Tsutsui, T. Matsui, R. Kikuchi, K. Eguchi, Appl. Catal. B: Environ. 81 (2008) 56.
[13] N. Kamiuchi, T. Matsui, R. Kikuchi, K. Eguchi, J. Phys. Chem. C 111 (2007) 16470.
[14] C. Gatel, E. Snoeck, Surf. Sci. 600 (2006) 2650.
[15] J.W.L. Wong, W.D. Sun, Z.H. Ma, I.K. Sou, J. Crystal Growth 227 (2001) 688.
[16] C.M. Woodbrige, X.J. Gu, M.A. Langell, Surf. Interface Anal. 27 (1999) 816.
[17] A.K. Datye, Q. Xu, K.C. Kharas, J.M. McCarty, Catal. Today 111 (2006) 59.
[18] R. -J. Liu, P.A. Crozier, C.M. Smith, D.A. Hucul, J. Blackson, G. Salaita, Appl. Catal. A: Gen. 282 (2005) 111.
[19] R. -J. Liu, P.A. Crozier, C.M. Smith, D.A. Hucul, J. Blackson, G. Salaita, Microsc. Microanal. 10 (2004) 77.
[20] T. Okanishi, T. Matsui, T. Takeguchi, R. Kikuchi, K. Eguchi, Appl. Catal. A: Gen. 298 (2006) 181.
[21] T. Matsui, K. Fujiwara, T. Okanishi, R. Kikuchi, T. Takeguchi, K. Eguchi, J. Power Sources 155 (2006) 152.
[22] T. Matsui, T. Okanishi, K. Fujiwara, K. Tsutsui, R. Kikuchi, T. Takeguchi, K. Eguchi, Sci. Tech. Adv. Mater. 7 (2006) 524.